NOTATION

$a, a_{(1)}, a_{(2)}$ = defined by Equations (23), (10), and (11)
$b_{(1)}, b_{(2)}$ = constants of integration in Equations (12) and (13)
$\mathbf{d}$ = rate-of-deformation tensor
$\mathbf{f}$ = body force vector per unit mass
F_z = physical component of force in z direction driving the fluid through the tube
$F_{z(i)}$ = F_z for phase i
p = pressure, defined for an incompressible fluid as $p = -1/3$ trace $(\mathbf{t})$
P = defined by Equation (9)
Q = voume rate of flow
r, z = cylindrical coordinates
R = radius of tube
$\overline{R}$ = radius of interface between the two phases
$\mathbf{v}$ = velocity vector
v_z = physical component of the velocity vector in z direction in cylindrical coordinates
$\mathbf{t}$ = stress, a second-order tensor
$t_{rr}, t_{\theta\theta}, t_{zz}, t_{rz}$ = physical components of $\mathbf{t}$ in cylindrical coordinates

Greek Letters

θ = cylindrical coordinate
κ = defined by Equation (4)
ρ = density
σ = surface tension
$\sigma_1 = \sigma_1(\kappa)$, $\sigma_2 = \sigma_2(\kappa)$, $\tau = \tau(\kappa)$ = material functions defined by Equations (1), (2), and (3)
τ = extra stress, a second-order tensor defined by $\tau = \mathbf{t} + p\mathbf{I}$ where $\mathbf{I}$ is the unit tensor
$\tau_{rr}, \tau_{\theta\theta}, \tau_{zz}, \tau_{rz}$ = physical components of τ in cylindical coordinates
τ^{-1} = single-valued inverse of τ which is assumed to exist (*4*, sec. 3)
φ = body force potential defined by Equation (5)

LITERATURE CITED

1. Gemmell, A. R., and Norman Epstein, *Can. J. Chem. Eng.*, **40**, 215 (1962).
2. Noll, Walter, *Arch. Rational Mech. Anal.*, **2**, 197 (1958).
3. Coleman, B. D., and Walter Noll, *ibid.*, **3**, 289 (1959).
4. ———, *Annals, N. Y. Acad. Sci.*, **89**, 672 (1961).
5. Coleman, B. D., *Arch. Rational Mech. Anal.*, **9**, 273 (1962).
6. Noll, Walter, *ibid.*, **11**, 97 (1962).
7. Coleman, B. D., and Walter Noll, *Phys. of Fluids*, **5**, 840 (1962).
8. Slattery, J. C., *Phys. of Fluids*, to be published.
9. Scriven, L. E., *Chem. Eng. Sci.*, **12**, 98 (1960).
10. Aris, Rutherford, "Vectors, Tensors, and the Basic Equations of Fluid Mechanics," Prentice-Hall, Englewood Cliffs, New Jersey (1962).
11. Slattery, J. C., *Chem. Eng. Sci.*, **19**, 379 (1964).
12. *Ibid.*, **19**, 453 (1964).
13. Serrin, James, "Handbuch der Physik," S. Flügge, ed., Vol. VIII/1, Springer-Verlag, Berlin (1960).
14. Bird, R. B., W. E. Stewart, and E. N. Lightfoot, "Transport Phenomena," Wiley, New York (1960).

Manuscript received January 13, 1964; revision received May 5, 1964; paper accepted May 6, 1964.

The Mechanics of Vertical Gas-Liquid Fluidized System I: Countercurrent Flow

A. G. BRIDGE, LEON LAPIDUS, and J. C. ELGIN

Princeton University, Princeton, New Jersey

Fluidized systems are encountered frequently in the chemical and petroleum industries in cases where it is necessary to transfer heat or matter from one phase to another immiscible or partially miscible phase or to carry out a chemical reaction on the surface of a catalyst. Because of the complexity of a detailed mathematical analysis, the designer of an industrial fluidized system must always rely on experimental data obtained from a small scale model of the system. A research program has been under way for a number of years at Princeton to develop a generalized theory of fluidized systems. It attempts to point out the similarities which exist between different fluidized systems so that data from one type can be used in the design of others. The program has been concerned with systems in which both phases move in a vertical direction, since this is the most common situation found in industrial equipment.

A. G. Bridge is with the California Research Corporation, Richmond, California.

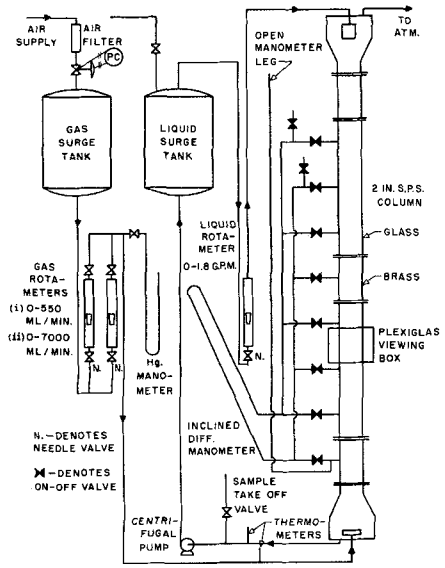

Fig. 1. Experimental apparatus.

In any fluidized system, interactions between the fluid and the particles tend to increase the drag force on each particle. This increase is most noticeable when the particles are close together, that is at high dispersed-phase holdups. The ability to predict the relationship between the relative holdups of the two phases and the phase flow rates in a system is essential for the design of such a system. Lapidus and Elgin (*11*) proposed that the relationship between the void fraction or holdup and the relative velocity between the two phases for a system of given geometry and physical properties was independent of the relative directions of motion of the two phases and of whether the particles were solid, liquid, or gaseous.

They defined relative velocity between the two phases or the slip velocity V_s as

$$V_s = V_f' - V_d' = \frac{V_f}{\epsilon} - \frac{V_d}{1-\epsilon} \qquad (1)$$

The convention that upward flow is positive was used with this definition. The generalized hypothesis can be stated mathematically as

$$V_s = \frac{V_f}{\epsilon} - \frac{V_d}{1-\epsilon} = f(1-\epsilon) \qquad (2)$$

where the functionality f depends purely on the geometry and physical properties of the system. With knowledge of the functionality f, the contact area between the phases and the pressure drop through the system can be estimated at any set of flow rates. Lapidus and Elgin (*11*) showed how a generalized diagram for a system could be constructed from this relationship.

The validity of the generalized theory has been investigated experimentally by a number of workers. Data, obtained with solid spheres in liquids, for the countercurrent (*12*), concurrent countergravity (*19*), and concurrent cogravity regimes (*13*) supported the hypothesis. With fluid droplets (*20, 1*) it was necessary to modify Equation (2) into the form

$$\frac{V_s}{V_T} = f_1(1-\epsilon) \qquad (3)$$

It was found that at high void fractions the relationship between V_s/V_T and $(1-\epsilon)$ for countercurrent flow was identical to the one which could be obtained from the analogous solid-liquid fluidized bed.

As expected, in all the countercurrent studies, at low void fractions, flooding caused the data to deviate from the batch fluidized data. A knowledge of the incidence of flooding in a fluidized system is required for its design, since the column diameter is determined by the maximum permissible velocities of the phases involved. There have been many attempts to predict this phenomenon and all have been based on the development of an analytical holdup-flow rate relationship to which is applied the flooding point criterion

$$\left.\frac{\partial V_d}{\partial(1-\epsilon)}\right]_{V_f} = 0 \qquad (4a)$$

Since the same flooding point arises regardless of whether V_f or V_d are varied, an equivalent criterion is

$$\left.\frac{\partial V_f}{\partial(1-\epsilon)}\right]_{V_d} = 0 \qquad (4b)$$

It was found that for the solid-liquid systems the holdup-flow rate relationship obtained from batch fluidized data was capable of predicting the flooding points in the countercurrent regime with the above criteria. In the case of fluid droplets (*1*), the data were inconclusive in this regard.

The generalized hypothesis, therefore, has been applied to all types of solid-liquid systems and also liquid-liquid systems, provided differences in terminal velocity behavior of solid and fluid particles were taken into account. The work reported here was concerned with its application to gas-liquid fluidized systems in which gas bubbles rose countercurrently through a flowing liquid. In this case another nonideality, namely the expansion of gas bubbles with decreasing hydrostatic pressure, was introduced.

A large number of investigators have studied gas bubble columns using a static water phase. As an illustration, Squires (*18*) has shown the qualitative similarity between some of these data and analogous fluidized bed data. Unfortunately, bubble sizes have not been recorded generally, and holdup values usually have included the region around the orifice, a location not typical of the behavior in the column proper. As a result, these data cannot be compared with the generalized theory.

Data previously obtained with countercurrent water flow (*17*) and with liquids other than water (*8*) are no better in this respect, although interesting qualitative observations are possible. In general, two different regimes have been observed, a laminar type of flow at low gas rates and a turbulent type of flow at higher rates (*17*). Liquid mixtures have tended to exhibit foaming in this latter regime.

The correlation of gas-liquid flooding points has had limited success, just as in the case for the liquid-liquid systems. Until Blanding and Elgin (*3*) introduced conical end designs, there was much uncertainty in the experimental measurements. Since then the definition usually used for flooding has been the point at which the dispersed phase starts to be rejected from the column proper. Sometimes this has been accompanied by a sharp change in holdup corresponding to the sudden formation of a second dense phase (*3, 12, 17*), but at other times it has occurred with no such sharp change. This is apparently at variance with the above flooding criteria, Equations (*4a*) and (*4b*).

EXPERIMENTAL

A schematic flow sheet of the apparatus is shown in Figure 1. Laboratory air was filtered and passed through a rotameter before being dispersed into the column by a stainless steel sparger. The continuous phase was recirculated through the system, a 25-gal. stainless steel surge tank being incorporated to minimize any temperature and concentration fluctuations.

Table 1. Details of the Experimental Runs

Run number	System	V_f, cm./sec.
W1	Air-water	0
W2	Air-water	1.65
W3	Air-water	3.33
W4	Air-water	5.41
IAA 1	Air-water + 10 p.p.m. isoamyl alcohol	0
IAA 2	Air-water + 10 p.p.m. isoamyl alcohol	2.23
IAA 3	Air-water + 10 p.p.m. isoamyl alcohol	3.90
IAA 4	Air-water + 10 p.p.m. isoamyl alcohol	5.41
GW 1	Air—58% glycerine solution	0
GW 2	Air—58% glycerine solution	0.78
GW 3	Air—58% glycerine solution	1.74
GW 4	Air—58% glycerine solution	2.66

The piping used for the liquid phase was ½-in. polyethylene tubing with polyethylene fittings. The temperature of both phases and the pressure of air at the rotameter were monitored.

The column test section was composed of Pyrex glass and brass pipe, both of 2-in. I.D. The end sections were made of Pyrex glass, and they included 16-deg. tapered sections (3). The column sections were flanged together with rubber O ring seals, and the end sections were flanged to ¼-in. brass end plates provided with connections for the entering and leaving fluids. Pressure taps were located about 9 in. from each other throughout the column. The taps were connected through a system of on-off valves to an inclined U-tube differential manometer. The manometer fluids used were carbon tetrachloride and air, in which case the manometer was inverted and inclined.

The bubble diameters were measured from photographs of the two-phase mixture. To minimize the distortion caused by the curved surface of the column, part of the column was enclosed in a transparent square box made from ⅛-in. plexiglas. The box was filled with the same liquid as in the column, and the photographs were taken through this box.

Tap water and a 58% glycerine-water mixture were chosen as the liquids because they give a different range of bubble diameters and because terminal velocity data of air bubbles in these liquids were available (5). The addition of 10 parts/million isoamyl alcohol to the water system was also investigated because this was known to alter the bubble diameter. The gas sparger was treated in hot nitric acid before being installed, and sufficient liquid was kept in the column to keep it submerged.

Runs were carried out at four different continuous phase rates (from 0 to 1.8 gal./min.) for each of the three liquids mentioned above. Before a run the gas was allowed to contact the recycling liquid for a period of 2 hr. so that both streams would be at the same temperature and the liquid would be saturated with air. When steady conditions prevailed, the pressure drop shown on the manometer was recorded for the seven column sections by manipulating the on-off valves. This was done in a random order, and the reading for one of the sections was always duplicated to give an idea of the reproducibility of the measurements. The flow rates, column pressure, air rotameter pressure, and phase temperature were recorded. Then the air flow rate was changed, and when steady conditions were obtained again, the procedure was repeated. Care was taken to maintain the top liquid level within the upper conical section.

Table 2. Location of Pressure Taps

Column position	Distance from sparger, cm.
1	35.0
2	57.25
3	79.70
4	103.15
5	124.80
6	146.70
7	168.70
8	192.20

Table 3. Physical Properties of Liquids Used

Liquid	Surface gravity (23° to 25°C.)	Surface tension, dynes/cm. (21°C.)	Viscosity, centipoises (25°C.)
Water	0.9987	72.9	0.8937
Water-IAA	0.9983	72.8	0.8937
Water-glycerine	1.1494	61.5-68.7	7.83

During the run, samples of the liquid were withdrawn for physical property measurements. The density was measured with a balance and the surface tension with a ring type of tensiometer. Also, photographs were taken of the bubbles at certain gas flow rates. Backlighting was used as suggested by Kintner et al. (10). Table 1 gives the continuous-phase flow rates used in each run, together with the run number which will be referred to frequently in the discussion of the results. Table 2 shows the distances between the porous plate and the various column pressure taps.

The temperature in all the experiments was 24° ± 2°C. The physical properties of the materials used are given in Table 3. These were determined from the samples taken during the experimental runs except for the viscosity values which were taken from the literature (6).

There was a wide variation of surface tension in the glycerine-water mixtures. It was noticeable that Run GW 4 (high continuous-phase rate) gave samples with high surface tensions (68.7), whereas Run GW 1 (stationary continuous phase) gave low values (61.5). The addition of 10 parts/million isoamyl alcohol did not affect the surface tension of the water.

RESULTS

The holdup data for typical runs are illustrated in Figures 2 to 4. In these charts, the gas holdup, or $(1 - \epsilon)$, is plotted against V_d^* which is the superficial gas flow rate, corrected to standard conditions of pressure (1 atm.). The wall friction pressure drop due to the flowing fluid was negligible compared with the holdup pressure drop because of the great density difference between the phases. As an illustration, the manometer deflection, when either air or liquid were flowing at maximum rate, was not measurable. The gas holdups are reported as point values at each pressure tap and were calculated from the arithmetic average of the observed pressure drops of the two sec-

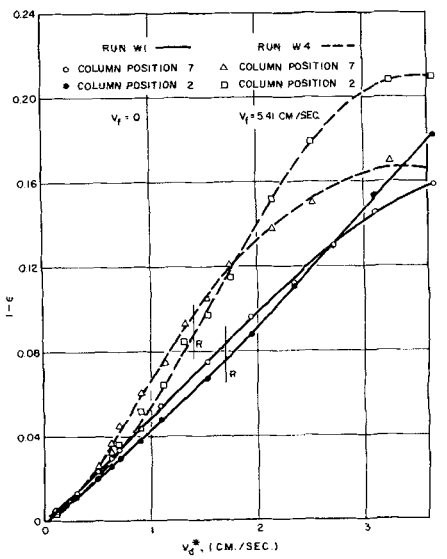

Fig. 2. Holdup data for air-water system.

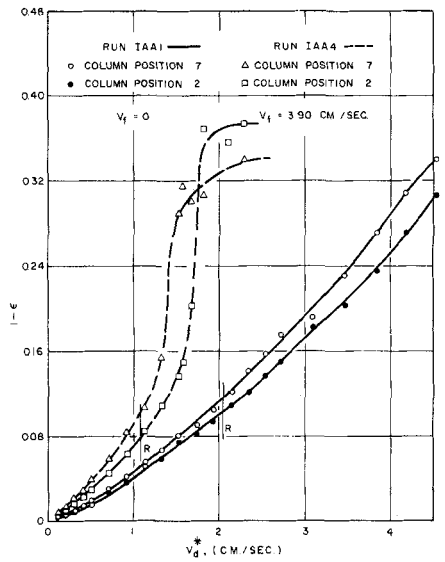

Fig. 3. Holdup data for air-water plus 10 parts per million isoamyl alcohol system.

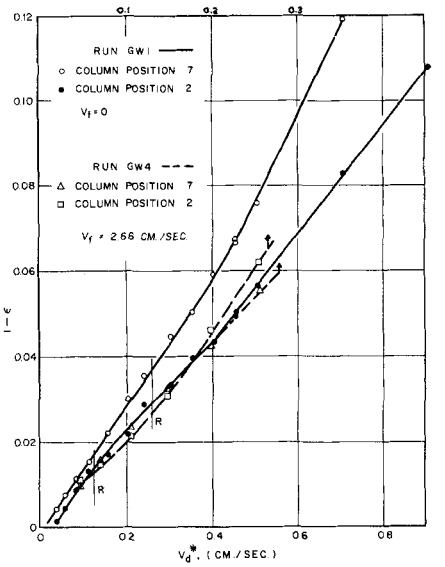

Fig. 4. Holdup data for air-water plus 58% glycerine system.

tions adjacent to the tap. The figures show only the data obtained for the bottom and top of the column. The other data fell between these extremes (2).

The major and minor axes were measured for about fifty bubbles on each photograph and the Sauter mean bubble diameter D_{BM} calculated. The bubble size distribution obtained by plotting this diameter against the volume fraction of the holdup composed of smaller bubbles was approximately Gaussian. The variation of bubble diameter with the gas flow rate is shown in Figure 5. The bubble diameters plotted here were obtained from the 50% point on the cumulative distribution plots, and each point represents the average of data taken from a number of photographs. No significant effect of liquid flow rate on the bubble diameter was found, although those obtained in Run W4 were higher than those in the other water runs. This was not thought to result from the higher liquid flow rates in Run W4, but rather because this run was carried out one month after the others and the nozzle was not treated before being used. The bubble sizes obtained in this run were not used in preparing Figure 5, although they were used in the analysis of the data.

The data points which were repeated during the water runs showed that the holdup values were reproducible to within 2 to 3% except at very low gas flow rates where differences of 10% were possible. The glycerine-water data showed more spread, but the holdup values were reproducible to within 5% over most of the range and to within 20% when the holdups were less than 0.01. The mean bubble diameters measured from many photographs taken at the same gas rate never deviated by more than 6% from their average, and generally the agreement was much better.

Water System

At low gas rates the bubbles rose uniformly, with each individual bubble following an oscillating path. When the rate was increased, the bubbles slowed down as their holdup increased, and the oscillations were gradually damped. At a particular gas flow rate some of the bubbles were rejected from the column into the conical end section of the gas inlet (point R on Figures 2 to 4). At this instant slight swirling occurred in the mixture at the top of the column. Further increases in gas rate caused a large quantity of bubbles to collect in the conical section. The bubbles as they entered the column proper tended to maintain this denser structure, and there was visually a higher gas holdup in the lower sections. In the upper sections, however, this structure broke down, and the swirling motion increased. Aggregates of bubbles or large bubbles seemed to move quickly up the center of the column, the bubbles near the wall being almost stationary. At high gas rates the whole column showed a violent churning action with large bubbles moving through the mixture fairly regularly. The pressure drop across the column sections fluctuated considerably, and averaged manometer readings were recorded. At low rates the small bubbles were ellipsoidal in shape with their major axes perpendicular to the column axis. The larger bubbles were often distorted considerably from this shape, but generally their major axes lay in the same direction.

Water-Isoamyl Alcohol System

The isoamyl alcohol caused much smaller bubbles to be produced at the sparger. They were generally ellipsoidal in shape with their major axes perpendicular to the column axis. At low rates of gas flow the bubbles rose steadily in vertical paths. Rejection was noticed, but the bed which formed in the conical section did not appear as stable as the bed of larger bubbles formed in the preceding runs. It seemed to pulsate, and its presence never gave the lower section of the column a substantially higher holdup than the rest of the column. No violent churning action was observed in the column, although after the point of rejection some bubbles seemed to move in aggregates, those near the wall sometimes moving

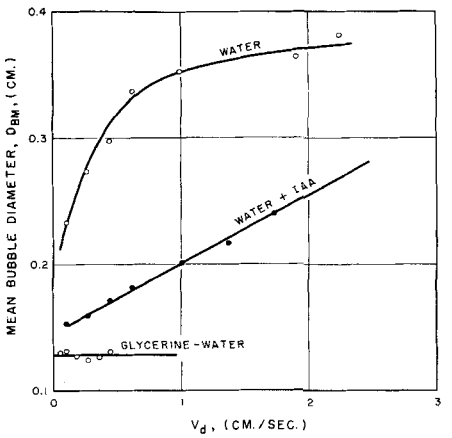

Fig. 5. Variation of mean bubble size with gas rate.

downward. At high liquid flow rates, after the point of rejection, a dense bubble bed was observed to move down the column with a sharp lower surface. Increasing either flow rate caused this bed to move down into the conical section where it stopped. Decreasing either flow rate caused it to move up the column. It was possible by keeping the flow rates steady to have the dense bed remain stationary in the upper half of the column for a period of at least an hour. As the liquid flow rate was decreased, this appearance of a dense bed at the top was less pronounced, and with a stationary liquid it was not observed at all. This system also had a tendency to foam at high gas rates, and it was important to maintain the upper liquid level in the enlarged section; otherwise the column would fill with foam.

Glycerine-Water System

This system behaved very similarly to the previous one except that the bubbles were smaller and practically spherical. The onset of rejection was more difficult to pinpoint exactly. However, it was found that if the liquid level were dropped into the 2-in. column, there was a definite gas flow rate at which foam formation at the surface started, and it seemed that this appearance of foam coincided with the start of rejection. Since the start of foam formation was much sharper than the onset of rejection, the conditions associated with it were recorded and are shown as point R in Figure 4. It was found that the position of the liquid level had no effect on the column holdup at low gas rates, but it was important to keep it in the expanded section at high rates because of the large quantities of foam which were formed. After the point of rejection, bubbles in the column seemed to move in aggregates, some moving downwards. At high rates, swirling started at the top, and a dense bed was observed to start moving downwards. It was impossible to continue in this condition since a great deal of foam was formed even with the upper liquid level in the expanded section.

DISCUSSION OF RESULTS

In all runs, up to the point of rejection (R), the gas holdup increased as the bubbles rose up the column, and the difference in holdup between the top and the bottom increased with increasing flow rate. After the point of rejection in the water system, the bubble bed which formed in the lower conical section influenced the lower part of the column so that the holdup in the lower sections increased. The holdup in the upper sections, however, did not increase to the same extent, and the holdup profile reversed itself. At higher gas flow rates the holdup at each point in the column reached a maximum, the lower part of the column having a higher holdup than the upper part. The results for the isoamyl alcohol and glycerine-water runs (Figures 3 to 4) did not indicate this sharp difference in behavior at the point of rejection. Even well beyond this point the holdup at the top of the column was greater than at the bottom. The results for Run GW 4 (Figure 4) showed some difference from this behavior, but these data were taken at such low holdups (0 to 0.06) that experimental error probably obscured the real holdup profile.

These differences in behavior are probably related to the ease with which bubble coalescence can occur in the different liquids. The water-isoamyl alcohol system produced much smaller bubbles than the water system, although there was no apparent difference in the measured physical properties of the two. It is likely that this difference in bubble sizes was due to the fact that as the bubbles were forming at the porous plate, coalescence between neighboring bubbles occurred in the water system, whereas the isoamyl alcohol inhibited this coalescence in some way. The fact that the isoamyl alcohol and the glycerine-water mixture exhibited foaming tends to indicate noncoalescing systems also. It was not possible to prove this point from the photographs, since at high gas holdups the bubble definition was poor. However, other workers have suggested that bubble coalescence was responsible for the turbulent conditions which arise at high gas rates with the water system (*17*).

One of the most interesting observations with the noncoalescing systems was the appearance of a dense bubble bed at the top of the column and its slow movement down to the bottom. This is shown graphically on Figure 3 for the isoamyl alcohol run, the holdup increasing very sharply with gas flow rate. Because of foam formation in the glycerine-water runs, it was not possible to obtain quantitative data above a certain gas flow rate, but there were definite indications that this system would have shown the same kind of behavior as the isoamyl alcohol one at higher rates.

In the case of the glycerine-water system the fact that foam formation started at a particular gas flow rate is reasonable, since foam will form when layers of bubbles arrive at the liquid-air interface faster than the layers can break up into spray on reaching this interface. This is, however, no reason for this to have happened under the same conditions which govern rejection of the bubbles from the column proper, although admittedly the actual mechanism of rejection is not understood. This coincidence was not noticed in the isoamyl alcohol runs, but the unstable nature of the foam with this system made observations of the incidence of foaming less reliable. At present then, no significance should be attached to this coincidence, although it would be worthwhile to study other systems in the light of these results.

Comparison of the Holdup Data With the Generalized Theory

The isoamyl alcohol system showed the widest variation in holdup, and so it provides a good test for the generalized theory. From the holdup and flow rate data the slip velocity was calculated at each point in the column for each of the four runs with Equation (2). The dispersed-phase flow rate V_d was based on the column conditions of pressure using the experimentally determined column pressure and extrapolating up the column with the aid of the holdup data. No temperture correction was applied, since the variation in temperature throughout the runs was slight. The mean bubble terminal velocity was estimated for each holdup determined by interpolating the data showing the variation of mean bubble diameter with gas flow rate (Figure 5) and then using the literature terminal velocity data (*5*). The terminal velocity data for tap water were used, and, as mentioned previously, the mean bubble diameter was taken as the 50% point on the cumulative distribution plots. The slip velocity ratio V_s/V_T was then plotted against the holdup $(1 - \epsilon)$. Figure 6 shows the results for column position 4 in each of the four isoamyl alcohol runs. Figure 7 shows the results for all column positions in one of the runs (IAA 3). The solid analogue with which they are compared was determined from the Zenz correlation of fluidized beds (*22*) at a particle Reynolds number of 500, which represents the average Reynolds number encountered in these runs.

Figure 6 shows that the slip velocity ratio is uniquely dependent on the holdup in the complete countercurrent regime for this system. In fact, this uniqueness exists even beyond the point of rejection. The data also follow quite closely the solid analogue, again even substantially past the point of rejection. The experimental points lie slightly

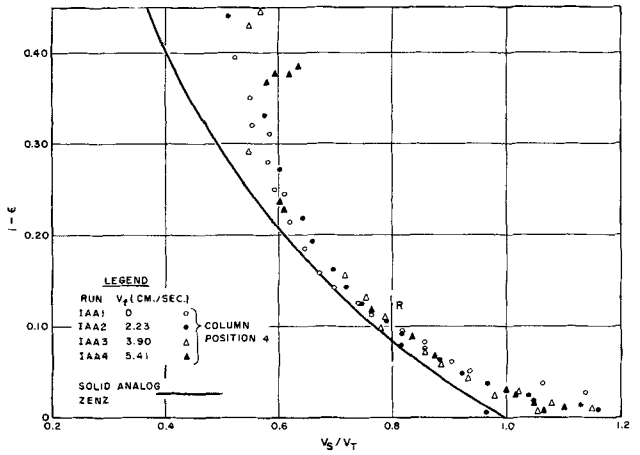

Fig. 6. Comparison of water-isoamyl alcohol system with solid analogue.

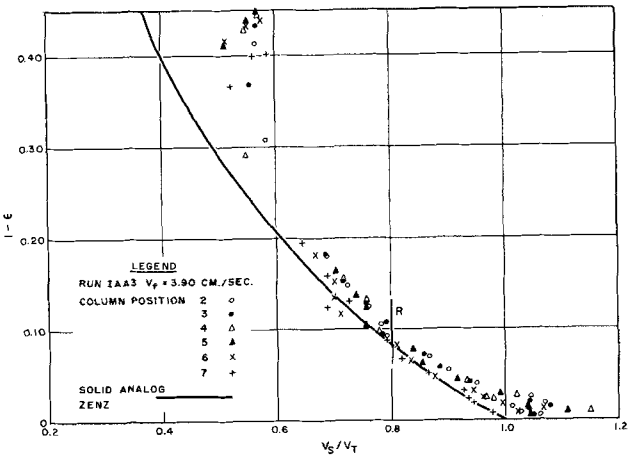

Fig. 7. Comparison of water-isoamyl alcohol system with solid analogue. Effect of column height.

above the solid analogue curve probably because inaccuracies in the terminal velocity data used in their analysis. Since the experimental data on this plot do not extrapolate back to $V_S/V_T = 1.0$ at $(1 - \epsilon) = 0$, that is when the bubbles are small, a correction for wall effect will not eliminate the difference. It is most likely that the terminal velocity of air bubbles in tap water differ from those when 10 parts/million of isoamyl alcohol are present. Haberman and Morton (5) have shown that the terminal velocity data of Gorodetskaya (4), measured in water containing small concentrations of various alcohols, can differ by as much as 10 to 20% from the tap water data.

Figure 7 shows that the effect of change in hydrostatic pressure in the bubble mixture is to maintain the same slip velocity ratio holdup relationships at all points. This follows from the fact that the data obtained from all column positions are correlated fairly well by one single curve. In plotting these data, no account was taken of the variation in the bubble diameter along the column length. The terminal velocity used in calculating the slip velocity ratio at any flow rate was the one corresponding to position 4 where the photographs were taken. This simplification is probably responsible for the fact that the data for the upper part of the column tend to lie below the data for the lower part on this graph.

Run IAA 3 was chosen arbitrarily for illustration in Figure 7, the other isoamyl alcohol runs giveng very similar results. The agreement with the generalized theory is excellent when one considers the possible errors in the terminal velocity values.

Figure 8 shows the data for the water system plotted as $(1 - \epsilon)$ vs. V_d. The solid analogue curves were calculated from the slip velocity ratio-holdup relationship given by the Zenz correlation, again at a Reynolds number of 500. The bubble terminal velocity used in the solid analogue was 23.5 cm./sec., since the major part of the water runs fell in the bubble diameter region where the terminal velocity had this constant value. Data for column positions 2, 4, and 7 are shown from Run W1. Below the point of rejection, all exhibited a unique dependence of holdup with the dispersed-phase flow rate. Since in this run V_f was zero, this is equivalent to saying that the slip velocity ratio-holdup relationship was unique at all points in the column. After the point of rejection, the data diverged from the analogue curve, and the data for the different parts of the column did not coincide. This was presumably because coalescence of bubbles occurred. To avoid complicating the diagram, only the results for column position 4 from the countercurrent runs are shown, and the data obtained above the points of rejection are not included. The data show reasonable agreement with the solid analogue below the point of rejection. Run W4 shows poor agreement at low flow rates owing to the fact that the bubble size measured in this run was noticeably larger than in the other runs. Slight disagreement could be expected for all the runs on this plot at low flow rates because a constant terminal velocity was used in the solid analogue. At zero gas flow rate the terminal velocity was about 21 cm./sec. instead of 23.5 which was used in the calculations.

The countercurrent data for the other column positions all obeyed the same slip velocity ratio-holdup relationship below the point of rejection. Above this point they were similar to the data of Run W1.

Figure 9 shows the data for the glycerine-water system. In this case the solid analogue curve was calculated with the assumption of a constant bubble terminal velocity of 6.5 cm./sec. The mean bubble diameter stayed within 6% of 0.128 cm. in the flow rate considered (see Figure 5), and so the error introduced by assuming a constant terminal velocity was not appreciable. The data for position 2 (the bottom of the column) are not included, since they were influenced by an end effect. At low gas flow rates for runs GW 1 and GW 2, the bubble chains produced at the sparger extended into the test section of the column producing lower holdups than those measured higher up the column. Only the data from column position 4 in the countercurrent runs are shown in Figure 9, and the solid analogue was calculated from the Zenz correlation at a

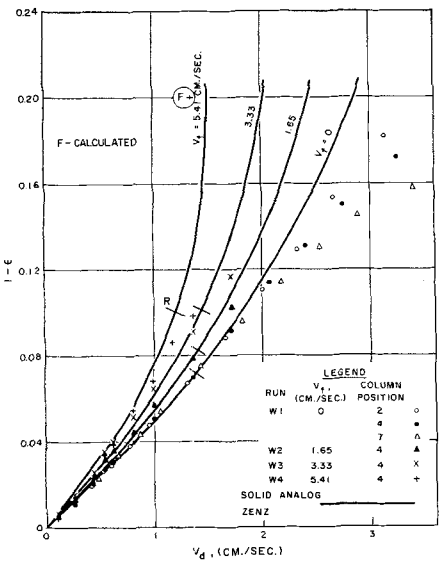

Fig. 8. Comparison of water system with solid analogue.

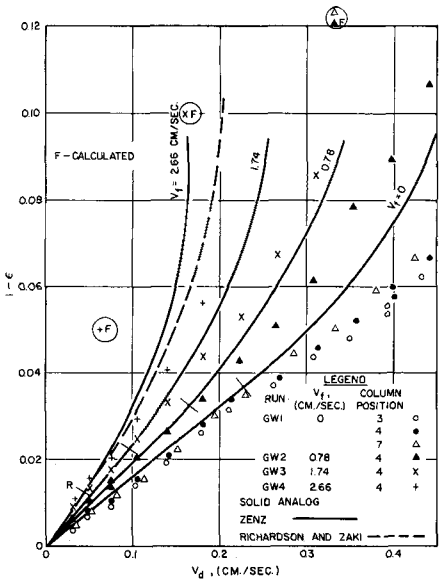

Fig. 9. Comparison of glycerine-water system with solid analogue.

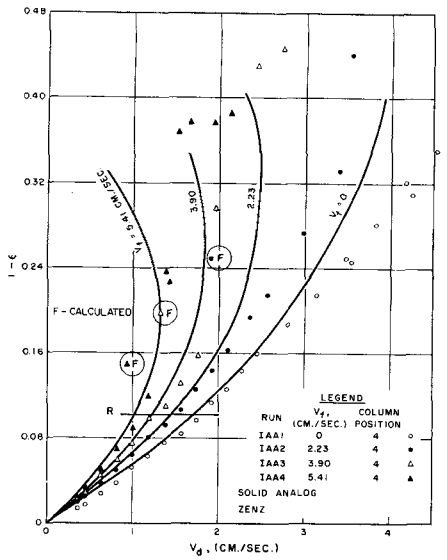

Fig. 10. Comparison of isoamyl alcohol system with solid analogue.

particle Reynolds number of 1.5. Again, below the point of rejection a unique relationship between the slip velocity ratio and holdup held for all the data shown. The data for Run GW 1 fell a little below the solid analogue, but this can also be attributed to errors in the terminal velocity used in calculating the theoretical curve. Although the assumption of constant terminal velocity is quite sound, the viscosity of the glycerine-water mixture used in these experiments was about 15% lower than that of the mixture reported (5) in the terminal velocity measurements (the viscosity varies very sharply with concentration in this range). As a result, it is probable that the terminal velocities of air bubbles in the mixture used in the present experiments were as much as 14% higher than the literature values. A correction of this magnitude would lower the solid analogue curve, giving better agreement with the data.

Above the point of rejection, the data for Run GW 1 diverged from the solid analogue, and the data from the different column positions spread out in the same manner as did the water data shown previously. Although the countercurrent data diverged considerably from the solid analogue after the point of rejection, the data from all positions in the column tended to follow closely the data for column position 4. [These data are not shown in the figure but are available (2)]. The data also, although being displaced from the solid analogue, still followed their general shape after rejection. They did not show the tendency for the rate of change of holdup with flow rate to decrease gradually. Since a dense bed started to appear at the top of the column at the high gas rates, it is probable that the data would have continued to follow the shape of the solid analogue. There is a lack of correlation of fluidized bed data in this Reynolds number range which is apparent when the experimental data are compared with the Richardson and Zaki correlation (*14, 15*) prediction (see Figure 9). As a result it is difficult to reach definite conclusions with this system. In general, however, it behaved like the isoamyl alcohol system in that it followed the solid analogue even after the point of rejection.

Comparison of Flooding Data With the Generalized Theory

To compare the flooding data with the theory it is most convenient to look at generalized plots of the data (Figures 8-9). The IAA system is represented in this fashion in Figure 10. All points designated *F* are calculated. In all cases the observed points of rejection (designated *R*) occurred at considerably lower flow rates than the generalized theory would have predicted. The predicted flooding point locus is based on the criterion that the slope of the curves on these plots is infinite. Rejection was always observed to occur before this point. Other data have shown this fact, and it casts some doubt on the usual approach to flooding point correlations of developing a realistic holdup-slip velocity relationship and applying the above criterion to it.

In solid-liquid, liquid-liquid, and gas-liquid systems, flooding has sometimes been accompanied by the formation of a dense bed at the dispersed-phase outlet which moved gradually through the column (*3, 12, 17*). Rejection of particles at the particle entrance was not observed before this happened, and so the point when the whole column was filled with the dense bed was taken as the true flooding point. This dense bed was observed in the present study at high continuous-phase flows with the noncoalescing systems, but, as the figures show, it appeared substantially after some bubbles had been rejected from the column into the feed section. This raises the question of which phenomenon represents the true flooding point.

Since both of these phenomena have been observed in a variety of systems, it is suggested that they are sufficiently general to be named *dispersed-phase flooding* and *continuous-phase flooding*. The former refers to rejection of particles at the dispersed-phase entrance, which occurs even when the continuous phase is stationary. The latter type of flooding refers to the appearance of a dense bed at the continuous-phase entrance which gradually moves through the column. This latter phenomenon has been observed only at high continuous-phase flow rates.

The generalized diagram (*11*) indicates that flooding is associated with the transition of a fluidized system from free countercurrent flow to a restrained fluidized bed through which particles continue to flow countercurrent to the fluid flow. Flooding will therefore be associated with transport of some of the particles against the effect of gravity. It has been shown (*7, 9, 16, 21*) that a batch fluidized bed is inherently unstable to fluctuations in void fraction. In fact, Jackson (9) has recently shown that the quality of fluidization (that is, particulate vs. aggregative) can be correlated with the stability of the system to these perturbations.

In a countercurrent system the local void fraction fluctuates, and as a result the local phase velocities can vary

widely. If a group of particles approach each other in the horizontal plane, they will be slowed down because the local fluid velocity between them increases. If a group of particles orientate themselves in a vertical plane, they will tend to decrease the fluid drag on each other and so will move faster than the average. At low dispersed-phase holdups, the distance between particles is sufficiently great that these effects do not interfere with the generally uniform flow picture. However, at high holdups it is conceivable that void fraction fluctuations can cause the local fluid velocity to exceed in places the local particle velocity with the result that some particles will be transported in the direction opposite to the effect of gravity. When this backflow of particles is noticeable, it creates a region of higher holdup, and thus the local fluid velocities are higher and more particles are affected. The particles probably change their relative configuration to minimize this effect, but under certain condition it is not possible for the disturbance to be damped out and flooding of the column will occur.

It is suggested here that continuous-phase flooding arises because of this instability. It appears at the continuous-phase entrance because the continuous phase is accelerating at this point and conditions are not as steady as in the column proper. It is noticeable from Figures 9 and 10 that this flooding coincides fairly well with the generalized theory flooding locus for the noncoalescing systems.

The incidence of dispersed-phase flooding cannot be predicted from the generalized theory. It is suggested that this phenomenon arises mainly because of the nonuniform particle-size distribution. It is natural that the smaller particles exhibit local transport at lower flow rates than the average. This will be noticed particularly at the dispersed-phase entrance because any particles transported into this section will be halted owing to the lower fluid velocities in the expanded section. The bed which forms here builds up on increasing either flow rate. It is, in effect, a restrained fluidized bed. The system within the column proper, however, is still quite stable, and one can operate in this flooded state provided expanded end sections are used. This is definitely a significant phenomenon in the behavior of the system, since it can herald coalescence of bubbles in gas-liquid systems and solids bridging with aggregative dumping in solid-liquid systems. Besides being dependent on the distribution of particle sizes, its incidence must also be a function of the stability of the system to void fraction fluctuations, since it arises even when there is zero net flow of the continuous phase. As a result, its prediction does not seem possible to present. It is suggested that with a uniform bubble-size distribution, dispersed- and continuous-phase floodup velocities would coincide in a single flooding velocity point.

In an effort to verify the above speculation, generalized theory flooding points were predicted from the bubble diameters given by the 5% point on the measured bubble size distributions. These calculations were identical to those used in obtaining the solid analogue curves in Figures 8 to 10 except that the smaller bubble diameter was used. The points at which these curves had an infinite slope are shown as Points F on Figures 8 to 10.

These calculations show that the maximum dispersed-phase throughput that a column can handle decreases very noticeably with decreasing bubble size. In fact, at high continuous-phase flow rates the predicted maximum rate, when the 5% bubble diameter is used, approaches the dispersed-phase rate at the observed point of rejection. The calculated holdup does not agree with the experimental value, and this is presumably because, although the smallest bubble diameter is important in describing this flooding phenomenon, an average bubble diameter must be used in describing the holdup conditions. Unfortunately, particle-size distributions have not been reported up to now in flooding studies. It would be of considerable value to carry out a flooding point investigation with solid particles of known nonuniform size distribution to see whether the generalized theory can be modified to account for this nonideality.

ACKNOWLEDGMENT

Financial assistance from the Esso Education Foundation, in the form of a fellowship to A. C. Bridge, was gratefully received during the course of this work.

NOTATION

V_d = superficial dispersed-phase velocity, (L/T)
V_d' = average particle velocity relative to walls, (L/T)
V_d^* = superficial dispersed-phase velocity, based on 1 atm. pressure, (L/T)
V_f = superficial continuous-phase velocity, (L/T)
V_f' = average fluid velocity relative to walls, (L/T)
V_s = slip velocity or relative velocity between the two phases, see Equation (2), (L/T)
V_T = particle terminal velocity, (L/T)
V_s/V_T = slip velocity ratio, (L/T)
ϵ = void fraction or volume fraction continuous phase
$1 - \epsilon$ = dispersed-phase holdup or just holdup
f, f_1 = functionalities
D_{BM} = average Sauter mean bubble diameter, (L)

LITERATURE CITED

1. Beyeart, B. O., Leon Lapidus, and J. C. Elgin, *A.I.Ch.E. Journal*, **7**, 46 (1961).
2. Bridge, A. G., Ph.D. dissertation, Princeton University, Princeton, New Jersey (1962).
3. Elgin, J. C., and F. H. Blanding, *Trans. Am. Inst. Chem. Engrs.*, **38**, 305 (1942).
4. Gorodetskaya, A., *Zh. fiz Khim.*, **23**, 71 (1949).
5. Haberman, W. L., and R. K. Morton, *Trans. Am. Soc. Civil Engrs.*, **121**, 227 (1956).
6. "Handbook of Chemistry and Physics," 36 ed., Chemical Rubber Publishing Co., Sandusky, Ohio.
7. Harrison, D., J. R. Davison, and J. W. de Kock, *Trans. Inst. Chem. Engrs. (London)*, **39**, 202 (1961).
8. Houghton, G., A. M. McLean, and P. D. Richie, *Chem. Eng. Sci.*, **7**, 40 (1957).
9. Jackson, R., *Trans. Inst. Chem. Engrs. (London)*, **41**, 13 (1963).
10. Kintner, R. C., et al., *Can. J. Chem. Eng.*, **39**, 235 (1961).
11. Lapidus, Leon, and J. C. Elgin, *A.I.Ch.E. Journal*, **3**, 63 (1957).
12. Price, B. G., Leon Lapidus, and J. C. Elgin, *ibid.*, **5**, 43 (1949).
13. Quinn, J. A., Leon Lapidus, and J. C. Elgin, *ibid.*, **7**, 260 (1961).
14. Richardson, J. R., and W. N. Zaki, *Trans. Inst. Chem. Engrs. (London)*, **32**, 35 (1954).
15. Richardson, J. F., and W. N. Zaki, *Chem. Eng. Sci.*, **3**, 65 (1954).
16. Rowe, P. N., *Trans. Inst. Chem. Engrs. (London)*, **39**, 175 (1961).
17. Shulman, H. L., and M. C. Molstad, *Ind. Eng. Chem.*, **42**, 1058 (1950).
18. Squires, A. M., *Chem. Eng. Progr. Symposium Ser. No. 38*, **58**, (1962).
19. Struve, D. C., Leon Lapidus, and J. C. Elgin, *Can. J. Chem. Eng.*, **37**, 141 (1958).
20. Weaver, R. E. C., Leon Lapidus, and J. C. Elgin, *A.I.Ch.E. Journal*, **5**, 533 (1959).
21. Wilhelm, R. H., and W. J. Rice, *ibid.*, **4**, 423 (1958).
22. Zenz, F. A., *Petrol. Refiner*, **36**, 147 (1957).

Manuscript received September 16, 1963; revision received July 8, 1964; paper accepted July 27, 1964.